Int. J. Heat Mass Transfer. Vol. 12, pp. 265–278. Pergamon Press 1969. Printed in Great Britain

GAS MIXING IN ROD CLUSTERS

V. R. SKINNER†, A. R. FREEMAN and H. G. LYALL

Central Electricity Generating Board, Berkeley Nuclear Laboratories, Berkeley, Glos., England

(*Received* 15 *November* 1967 *and in revised form* 7 *September* 1968)

Abstract—Transverse temperature differences in a coolant flowing axially along a rod cluster or tube bundle will be reduced by diffusion of heat from one sub-channel to another through the gaps between the rods or tubes. This process, called mixing for convenience, has been studied experimentally using a mass-transfer analogy. Mixing rates were found to be greater than can be explained by turbulent diffusion theory. They were attributed to the action of secondary velocities. The results are used to predict the extent to which mixing will reduce temperature differences within fuel clusters of Advanced Gas-Cooled Reactors.

NOMENCLATURE

A, Constant in expression for concentration decay with Reynolds number;
A_f, channel flow area [ft^2];
Cp, specific heat (CHU/lb°C);
E_M, effective diffusivity [ft^2/sec];
Q_r, volumetric flow rate in rth sub-channel;
Q_T volumetric flow rate in whole channel;
M, mixing coefficient;
Re, Reynolds number $W_T de/\mu A_f$;
St_g, gap Stanton number $h_g/\rho\bar{\bar{u}}Cp$;
St'_g, gap Stanton number for mass transfer $n_g/\bar{\bar{u}}(\bar{c}_1 - \bar{c}_2)$;
W_T, total channel mass flow [lb/s];
W_r, sub-channel mass flow;
c_r, N_2O concentration in rth sub-channel;
de, equivalent diameter [ft];
h_g, gap heat-transfer coefficient [CHU/s ft^2 °C];
l, Axial distance from point in channel to channel inlet [ft];
n, nitrous oxide flux;
q, Heat flux;
q_r, Heat input per foot into sub-channel r;
s, Gap width [ft];
u, axial velocity [ft/s];
u^*, friction velocity;
v, secondary flow velocity [ft/s];
v', turbulent velocity component [ft/s];
x, axial co-ordinate [ft];
x^*, axial distance for diffusion through rod gap [ft];
y, distance from channel wall [ft];
$\hat{y}$, distance from channel wall to surface of no shear [ft];
α, γ, constants in concentration decay expression;
ρ, fluid density [lb/ft^3];
θ_r, mean gas temperature in rth sub-channel;
$\theta_r(x)$, gas temperature at axial location x in rth sub-channel;
θ^*, rate of change of temperature difference when no mixing occurs, $\dfrac{q_r - q_{r+1}}{W_r Cp}$;
μ, fluid viscosity [lb/ft sec].

Subscripts

g, refers to gap region;
r, refers to rth sub-channel;
o, indicates conditions at the position of the injector;
1, indicates conditions in inner sub-channel of cluster;

† Now at Delaney Gallay Limited, Burton-on-Trent.

2, indicates conditions in outer sub-channel of cluster.

Overbars

–, denotes a sub-channel mean quantity;

=, denotes an overall channel mean quantity.

1. INTRODUCTION

THE FUEL element for the Advanced Gas-Cooled Reactors being built for the G.E.G.B. at Dungeness will be a cluster of 36 fuel rods in a circular channel. Thus the coolant flow passages will consist of a number of sub-channels inter-connected by the gaps between the rods. As the reactor coolant gas flows along the channels, temperature differences will develop between the gas in the various sub-channels. In particular, the axial temperature gradient in the gas flowing in the outermost sub-channel of the cluster, because of the presence of the unheated channel wall, will be lower than that in the gas flowing in the inner sub-channels. There will thus be a gradually increasing temperature difference between sub-channels along the cluster. This effect is illustrated in Fig. 1 which shows typical gas temperature profiles for outer and inner sub-channels in an axi-symmetric cluster. In fact the sub-channels of such a cluster are not completely separated. Transfer of heat will occur from hot sub-channels to cooler sub-channels through the rod gaps and also through the rods themselves. Thus in practice the net temperature difference between sub-channels will be reduced as shown in Fig. 1.

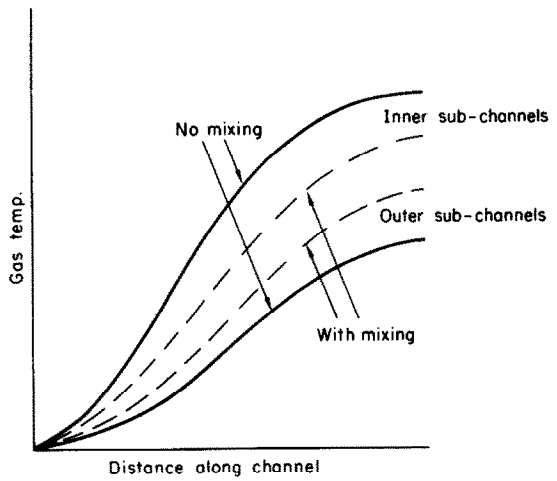

FIG. 1. Typical gas temperature profiles in the sub-channels of a rod cluster.

This paper gives the results of an experiment to measure the rate of transfer of heat between sub-channels, calling mixing, using a mass transfer analogy. It shows that the mixing, which is much stronger than can be explained by turbulent diffusion, is able to reduce significantly local temperature differences. However, it is not strong enough to reduce adequately temperature differences occurring right across a cluster.

2. THE EXPERIMENT

Because of the experimental difficulties in measuring very small differences in gas temperatures with sufficient accuracy, and of allowing for the effects of conduction in the pins and the channel wall it was decided from the outset not to attempt a direct measurement of the mixing of heat. These experimental difficulties can be avoided by using nitrous oxide as a tracer in air as an analogy for heat. A justification for this technique has been given by Hall and Hashimi [1].

In many heat-transfer experiments a heat flux is applied which does not vary along the length of the duct giving, after an adequate inlet length, a constant heat transfer coefficient and a constant shape to the temperature profile. In a duct consisting of inter-connected sub-channels, the inlet length required to give these fully developed conditions can be very long, and in a mass-transfer experiment with constant wall flux, would lead to very large total injection rates. No attempt was made to achieve this type of fully developed conditions. Instead, injection was concentrated over a very short axial distance, about 0·050 in, and the concentration distribution at various points downstream was measured.

To avoid the necessity for much laborious sampling with small tubes, large representative samples of the flow were taken isokinetically to give information on the mean concentration in complete subchannels at various planes downstream of the injector.

A limited amount of traversing was done with sampling and pitot tubes to give detailed information on flow and concentration distributions.

3. APPARATUS

The apparatus consisted of a smooth duct 5·683 in. dia. and 13 ft long. It is shown schematically in Fig. 2. The layout of the cluster can be

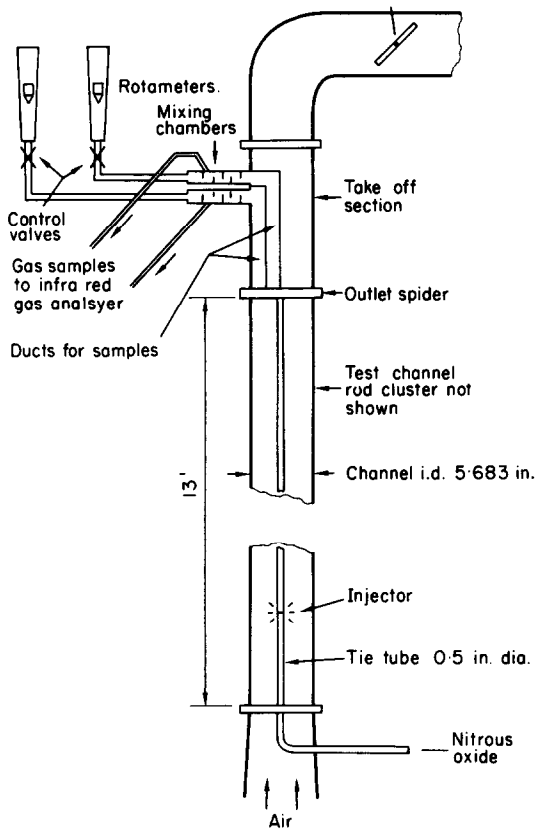

FIG. 2. Schematic diagram of apparatus.

seen in Fig. 3. Two types were tested; one consisted of 6 smooth rods 1·35 in. dia. on a 3·625 in. P.C.D. and the other of 6 roughened rods with the same root diameter on the same P.C.D. The roughness consisted of square ribs 0·015 in. high pitched at 0·11 in. A smooth 0·5 in. dia. stainless steel tube (the tie tube) passed through the middle of the cluster. The nitrous oxide injector was a line source round the tie tube. Its distance from the sampling plane (the mixing distance) could be varied. The sampling plane was situated at the cluster outlet.

The take-off (or sampling) section, immediately downstream of the outlet spider, was designed to duct away separately one sixth of the flow in the inner region and one sixth of the flow in the outer region, as shown in Fig. 3. Pitot-static probes were mounted in the outlet spider, Fig. 3. The flow rate of the sampled flows could be varied by means of the control valves shown. Iso-kinetic sampling was achieved by balancing the readings from the like pairs of pitot-static probes. The sampled flows were led via mixing chambers and the control valves to separate rotameters. The gas concentrations were measured using a Hilger I.R.D. i.r. gas analyser using samples led from the mixing chambers. Static pressure readings were taken at 1 ft intervals along the test section. The pressure tapping bosses could be replaced by micrometer traversing gear for velocity or gas concentration measurements.

Air at flow rates up to 2 lb/sec was supplied to the test section from a centrifugal blower. The flow rate was measured on an orifice plate designed to B.S. 1042.

4. COMMISSIONING

4.1 *Flow development*

Velocity traverses were made along a radius between two adjacent rods at 1 ft intervals along the test section. It was found that after an inlet length of 4 ft ($l/de = 35$) the profiles were all similar in shape, the maximum differences in local velocity at any point being of the order of 3 per cent. Traverses at the last position with and without the take-off section in place did not differ significantly indicating that any disturbance caused by the take-off section was propagated less than 1 ft upstream.

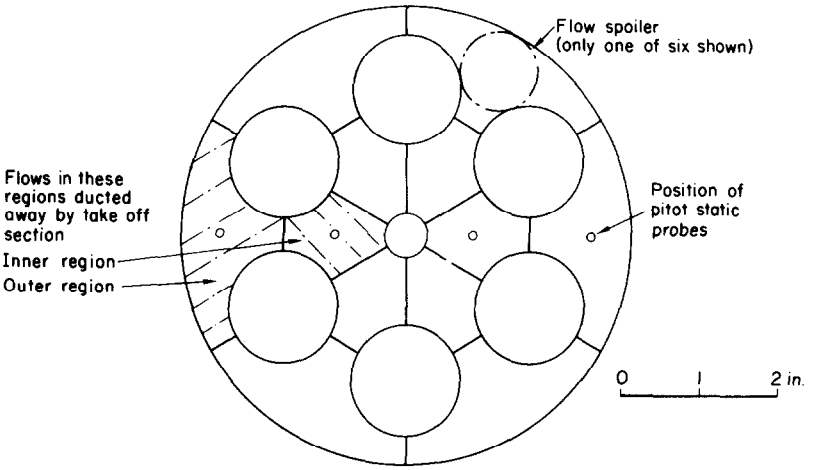

FIG. 3. Layout of cluster showing flow regions sampled and positions of pitot static probes used to obtain iso-kinetic samples.

4.2 *Flow distribution*

With the take-off section removed pitot-static probes were traversed throughout an entire sixth section of the cluster. These measurements were carried out on both the smooth and the roughened clusters. By plotting the results in the form of a velocity contour map, Fig. 4, it was possible to evaluate the ratio of the outer sub-channel flow rate to the inner sub-channel flow rate. This was found to be 1·67 for the smooth cluster and 1·70 for the roughened cluster. It was expected that a larger proportion of the flow would flow in the outer sub-channel with the roughened pins because the channel wall was smooth. However, this difference measured is probably barely significant.

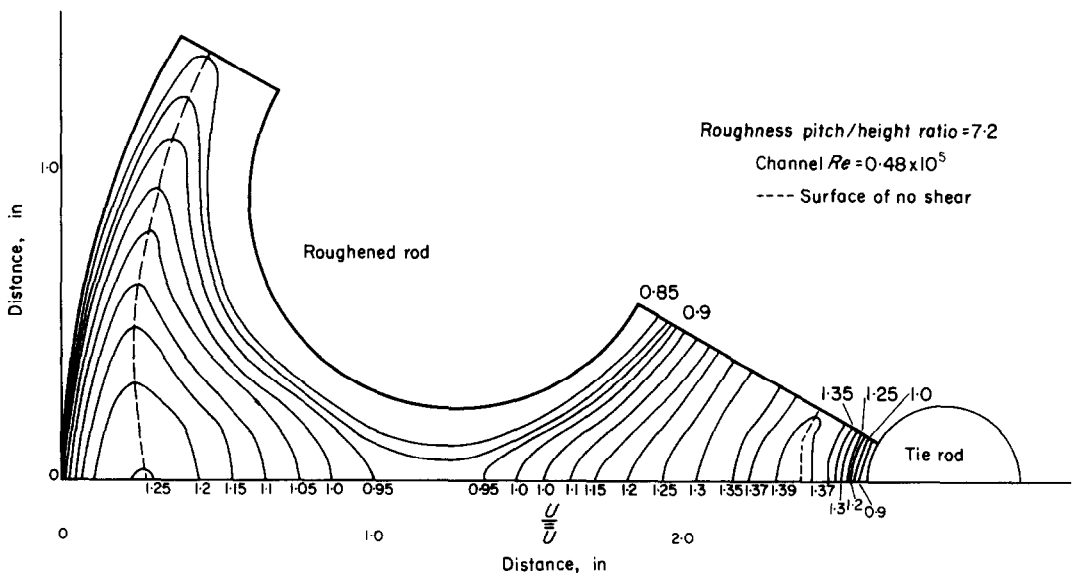

FIG. 4. Velocity contours in the roughened rod cluster.

4.3 *Sampling technique*

It was important to be certain that the sampling technique used was truly isokinetic, and that the outlet spider and take-off section did not cause azimuthal or radial deflection of the flow before it was sampled. The former was checked by comparing the sampled flow rate with one sixth of the total flow rate measured by the orifice plate. Agreement was within 2 per cent, which was considered to be very good. However, it was found that the ratio of the outer sub-channel flow to the inner sub-channel flow given by the flow through the take-off section was 2·15 for the smooth cluster, compared with 1·7 obtained from the detailed traverses made 1 ft upstream of the outlet spider described in section 4.2.

This discrepancy between flow distribution at the sampling plane and a position 1 ft upstream was due to the outlet spider displacing flow from the inner to the outer sub-channel. This disturbance was prevented by inserting flow spoilers in the outer region of the spider, one of the six is shown in Fig. 3.

For all experimental runs, comparison between the sampled flow rate and one sixth of the flow rate measured by the orifice plate were made, as were checks on the ratio of flow rates in the inner and outer regions. In addition to these air flow balances, nitrous oxide balances were obtained by comparing the sampled rate with one sixth of the injected rate as a check on the experimental accuracy. During the tests air balances of 3 per cent and nitrous oxide balances of 10 per cent were regarded as satisfactory.

5. FLOW MIXING

5.1 *Procedure*

The procedure during these tests was the same for both the roughened and smooth rod clusters. With the injector in the topmost position (3·85 ft from the take-off section) the channel mass flow was set at the lowest convenient rate. When a steady rig temperature had been attained the pitot-static heads in the outlet spider were balanced to ensure isokinetic sampling and readings were taken of orifice plate temperature, static and differential pressure and the inner and outer zone flow rates. The mean nitrous oxide concentration of the inner and outer flow regions and the total amount of nitrous oxide injected were also recorded. From these readings air and nitrous oxide balances were determined and the values of Reynolds number and the normalized concentration decay evaluated. The Reynolds number is defined by $Re = (W_T de/\mu A_f)$ where W_T is the total channel mass flow rate and de and A_f are based on the total wetted perimeter and flow area. For the roughened cluster, flow areas and perimeter corresponding to the root diameter of the rods were taken.

The normalized concentration decay is defined by $[(\bar{c}_1 - \bar{c}_2)/(\bar{c}_1 - \bar{c}_2)_0]$ where $\bar{c}_1$ and $\bar{c}_2$ are the mean nitrous oxide concentrations in the inner and outer flow regions respectively, as measured in the sampled flows. The subscript 0 refers to concentrations at the position of the injector.

The above readings were repeated for a number of flows covering the range $Re = (0{\cdot}2\text{–}0{\cdot}8) \times 10^5$. A total of six injector positions was investigated for the smooth cluster and five for the roughened cluster.

5.2 *Results*

The results expressed as a normalized concentration decay $[(\bar{c}_1 - \bar{c}_2)/(\bar{c}_1 - \bar{c}_2)_0]$ are shown plotted against Reynolds number for each injector position in Figs. 5 and 6. The straight lines obtained show that over the range considered $[(\bar{c}_1 - \bar{c}_2)/(\bar{c}_1 - \bar{c}_2)_0] = ARe^n$. The values of log A and n are plotted against x, the distance of the point of injection from the sampling plane, in Figs. 7 and 8.

Before any mass transfer can take place through the gaps, and hence be detected in the experiment, the nitrous oxide must diffuse across the inner region. By extrapolation of the lines on Figs. 7 and 8 it was found that the nitrous oxide was convected an axial distance of 2·25 ft while diffusing across to the gap. This distance could be assumed constant over the Reynolds number range of the experiment. This leads to,

$$n = \alpha x^* \qquad A = e^{\gamma x^*}$$

where $x^* = (x - 2{\cdot}25)$ ft.

The smooth cluster results show a discontinuity between $x = 5{\cdot}85$ ft and 6·85 ft. This is due to the effect of the centre spider. If an additional channel length of 5 in. is allowed for this spider the discontinuity disappears. No disconuity was observed in the case of the roughened rods.

Thus the empirical expression for the decay of an initial concentration difference across the gap region of the simple cluster may be written:

$$\frac{(\bar{c}_1 - \bar{c}_2)}{(\bar{c}_1 - \bar{c}_2)_0} = e^{\gamma x^*} Re^{\alpha x^*}$$

where α smooth = 0·013, α rough = −0·054, γ smooth = −0·184 and γ rough = 0·462.

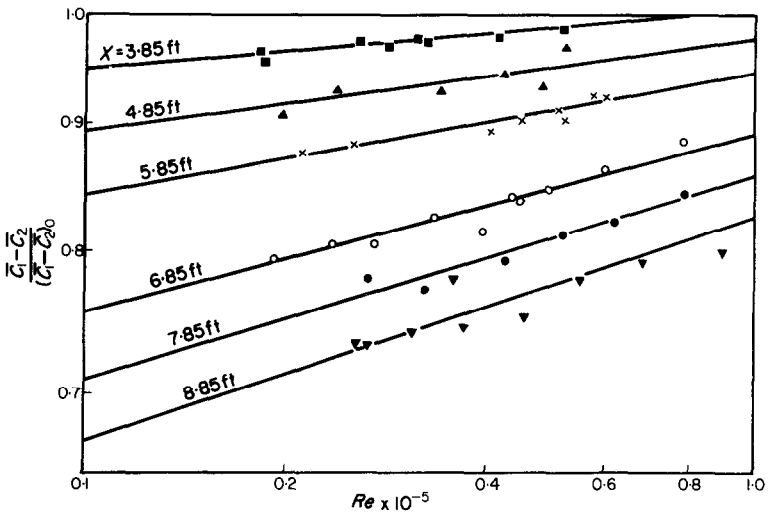

FIG. 5. Variation of normalized concentration decay with Reynolds number—smooth rod cluster.

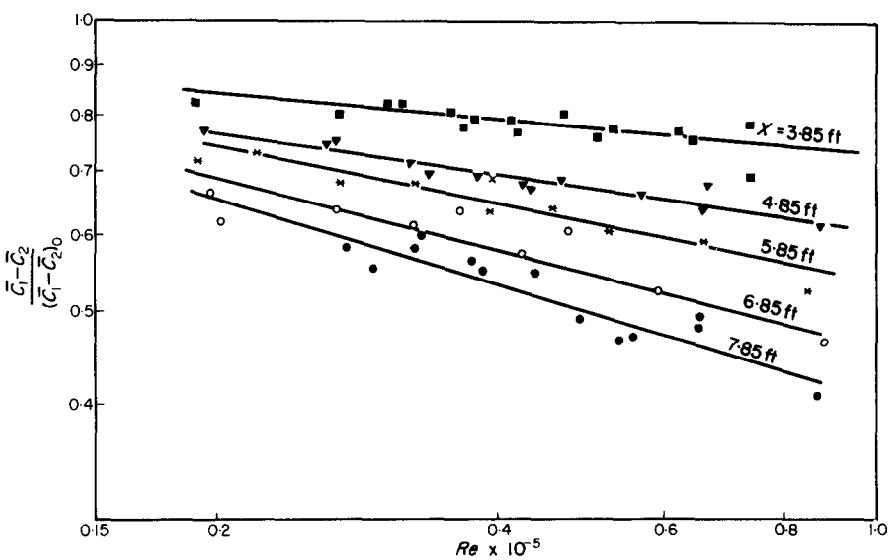

FIG. 6. Variation of normalized concentration decay with Reynolds number—roughened rod cluster.

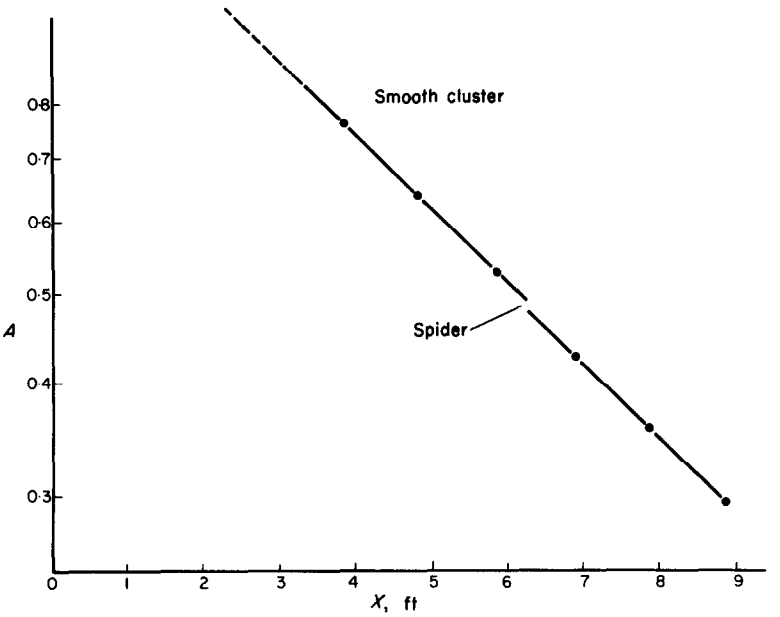

FIG. 7. Variation of constants A and n with axial distance—smooth rod cluster.

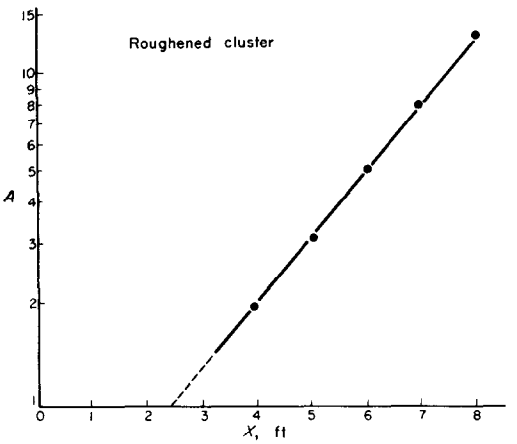

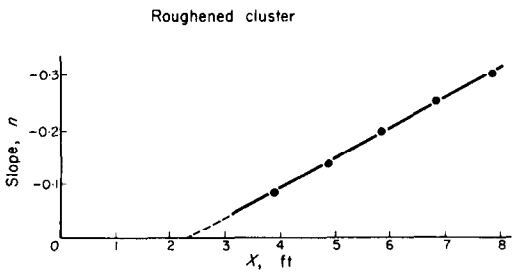

FIG. 8. Variation of constants A and n with axial distance roughened rod cluster.

6. DERIVATION OF GAP STANTON NUMBER

The rate of heat transfer through the gaps from one region to the other can be conveniently described in terms of a gap Stanton number defined by:

$$St_g = \frac{q_g}{Cp\,\rho\bar{\bar{u}}(\bar{\theta}_1 - \bar{\theta}_2)}.$$

Similarly a Stanton number for mass transfer can be defined:

$$St'_g = \frac{n_g}{\bar{\bar{u}}(\bar{c}_1 - \bar{c}_2)}$$

where nitrous oxide concentrations and fluxes are both expressed in the same terms; i.e. mass or volume.

It is shown in Appendix I that the empirical expression for concentration decay leads to:

$$St'_g = -0{\cdot}116\{\gamma + \alpha \log_e Re\}$$

over the range of Re considered.

It follows from the form of the concentration decay expression that St'_g is independent of x, as one would expect.

The gap Stanton number for the rough and

smooth assemblies as given by the above expression is shown plotted in Fig. 9.

7. ANALYSIS OF CONCENTRATION PROFILES

Skinner [2] analysed the results of concentration traverses taken during earlier flow mixing tests on the smooth cluster. The results of these tests are not included in this paper because circumferential variations in nitrous oxide injection rate were unacceptably large in some cases. He defined an effective diffusivity, E_M, in the gap for mass transfer by:

$$n_g = -E_M \left(\frac{\partial c}{\partial y}\right)_g.$$

We also have in the gap region, if E_M is constant in that region:

$$u \frac{\partial c}{\partial x} = E_M \frac{\partial^2 c}{\partial y^2}.$$

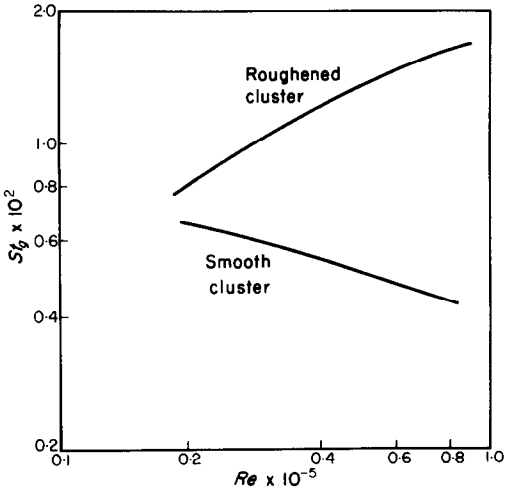

FIG. 9. Gap Stanton number obtained from concentration measurements.

Using the results of his concentration traverses and both the above equations in finite difference form Skinner derived the following values of E_M at a Reynolds number of $0{\cdot}4 \times 10^5$: 0·037, 0·037, 0·048, 0·033, 0·033, 0·040 and 0·037 ft^2 sec^{-1}. The different values were obtained from analyses at different axial stations.

Rapier [3] has suggested the expression $0{\cdot}1\ \mu^* \hat{y}$ for eddy diffusivity for momentum. This expression gives a value 0·006 ft^2 sec^{-1} in the gap region and 0·038 ft^2 sec^{-1} in the inner flow region away from the gaps. Rapier's expression gives a higher value of eddy diffusivity than other workers' but it is still significantly lower than the effective diffusivity in the gap region found by Skinner [2]. This suggests that the rate of transfer of nitrous oxide through the gap is greater than can be accounted for by turbulent diffusion alone.

Skinner [2] also analysed concentration profiles in the inner flow region away from the gaps. He found that the behaviour could be explained by turbulent diffusion using an acceptable value of eddy diffusivity. The higher rate of diffusion in the gap region is attributed to a secondary flow.

8. A SECONDARY FLOW MODEL FOR THE GAP STANTON NUMBER

8.1 *Discussion of secondary flow and turbulence measurements*

Measurements by a number of workers have shown that in turbulent flow in straight non-circular parallel ducts secondary flows will occur. Nikuradse [4] made measurements in a number of different ducts including one rather similar to the gap region between rods. He inferred, from his axial velocity measurements and from flow visualization tests that a secondary flow occurred in the gap region—see Fig. 10(c).

More recently, Gessner and Jones [5] from their measurements in smooth square and rectangular ducts showed that the magnitude of the secondary flow reduces with increasing Reynolds number. Peak local values of secondary velocity approaching 2 per cent of the centre line velocity were measured. Typical values are 1 per cent at $Re = 0{\cdot}75 \times 10^5$ falling to 0·7 per cent at $Re = 3 \times 10^5$. Hoagland [6] and Brundrett

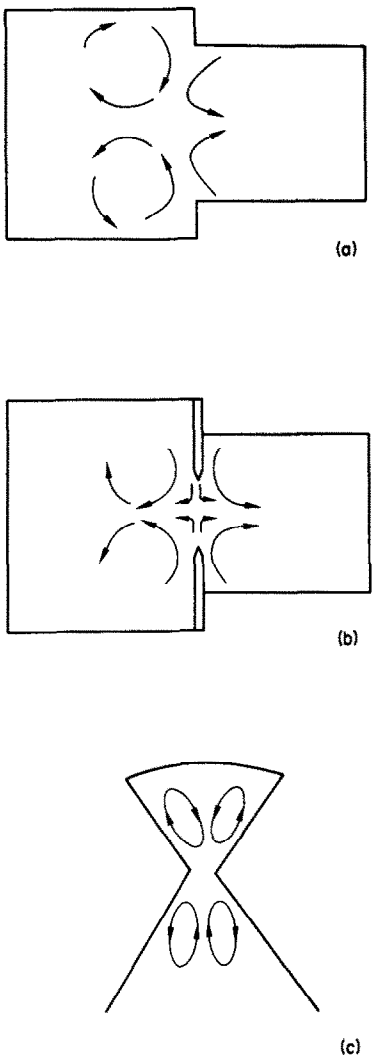

FIG. 10. Secondary flow patterns in various ducts.

and Baines [7] measured similar secondary flows to Gessner and Jones [5]. Hoagland [6] found that close to the wall, the magnitude of the secondary flow, expressed as a percentage of the primary flow, decreased with increasing Reynolds number.

Secondary flow measurements have been made in this laboratory in a stepped rectangular duct having two configurations, Fig. 10. Secondary flows of up to 3 per cent were found in configuration (a) and up to 4 per cent in configuration (b). An average value for the gap region is 2 per cent. These secondary flows, which flow from the wall into the gap region are in the opposite direction from the suggestions of Nikuradse [4].

If it is accepted that the driving force for the secondary flows arises from the distribution of the transverse turbulent velocity fluctuations, then it is reasonable to accept that the secondary flow, expressed as v/u should vary in a similar manner to the turbulent fluctuations expressed as v'/u. Measurements of this latter parameter in a circular pipe by Kjellström and Hedberg [8] show a significant falling off with increasing Reynolds number. This lends support for Gessner and Jone's [5] finding that secondary flow falls off with increasing Reynolds number in a smooth duct. Hanjalic and Launder [9] at Imperial College in a high aspect ratio duct with one wall roughened measured values of v'/u of 18 per cent independent of Reynolds number. This compares with about 3 per cent measured by Laufer [10] in smooth pipe flow.

From the results of the secondary flow measurements of Fig. 10 it would not be unreasonable to expect secondary flows of about 2 per cent in the smooth rod cluster, and considerably higher in the rough cluster because of the higher turbulence intensity. One would expect the secondary flow to fall with increasing Reynolds number in the smooth cluster, but to be sensibly constant in the rough cluster, once the Reynolds number is high enough for fully rough conditions to be established. At lower Reynolds numbers one would expect secondary flow rate to increase with increase in Reynolds number for the rough cluster.

8.2 *The secondary flow model*

In Fig. 11 the proposed secondary flow model is shown. Fluid at temperature $\bar{\theta}_1$ in region 1 is carried towards the gap by the secondary velocity $\bar{v}$, and fluid at temperature $\bar{\theta}_2$ in region 2 is also carried towards the gap by secondary

velocity $\bar{v}$. These two streams are assumed to mix in the gap region and fluid flows out of the gap region at temperature $(\bar{\theta}_1 + \bar{\theta}_2)/2$ as shown. Note that the directions of the arrows can be reversed without affecting the argument. If s is the gap width, then the rate of heat flow through the gap is

$$\frac{\rho C p \bar{v} s}{2}\frac{(\bar{\theta}_1 - \bar{\theta}_2)}{2} = s q_g$$

therefore,

$$St_g = \frac{q_g/(\bar{\theta}_1 - \bar{\theta}_2)}{\rho C p \bar{u}} = \frac{\bar{v}}{4\bar{u}}.$$

If the secondary flow in the gap region is of the order of 2 per cent, then St_g should be about 0·005. This value agrees well with the mixing measurements for the smooth cluster. For the rough cluster a secondary flow of 6 per cent at the highest Reynolds number is required if the above model is to predict the measured mixing rate. Although this value seems high, it is not out of the question in view of the 18 per cent turbulence intensity measurements of Hanjalic and Launder already referred to.

9. APPLICATION TO REACTOR CONDITIONS

In order that the results obtained in the 6-pin cluster experiments could be applied to actual fuel element clusters of up to 36 rods a theoretical assessment of mixing was made. To ease the analysis it was necessary to make a number of simplifying assumptions, but general conclusions can be drawn from the calculations with some confidence.

The details of the analysis are given in Appendix II. It considers mixing in arrays of up to seven adjacent sub-channels; thus the results do not apply directly to clusters in circular channels. However, it seems reasonable to assume that the seven sub-channels case is similar to mixing right across a 36 rod cluster, see Fig. 12. For mixing between the centre and the outside of the cluster the three-sub-channels case probably gives a good indication of mixing rates.

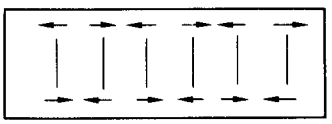

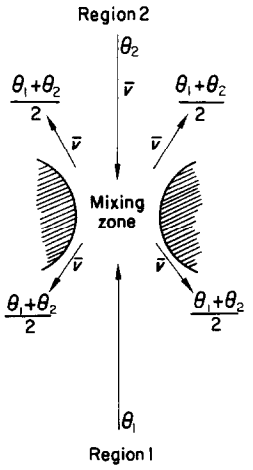

FIG. 11. Secondary flow model.

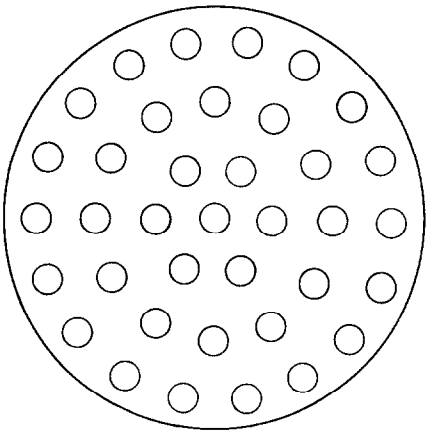

FIG. 12. Similarity between 7 sub-channel flow model and a 36 rod cluster.

It is assumed that fluid enters the sub-channels at a uniform temperature and that the mass flow rate W_r is the same for each sub-channel. Because of differences in surface heat flux in the various sub-channels, temperature differences between the sub-channels will develop in the fluid as it flows along the array. These temperature differences will be reduced by mixing.

The results of the analysis are given in Fig. 13

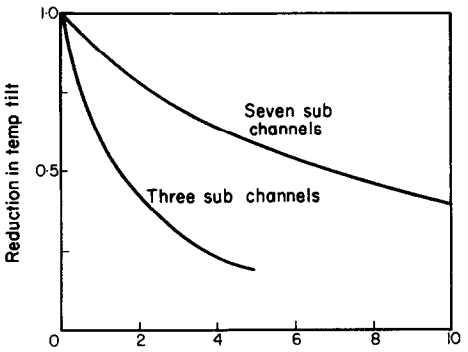

FIG. 13. Reduction in temperature difference across 3 and 7 sub-channels.

where the reduction in temperature difference across the various arrays of sub-channels is given against length. Length is measured in units of W_rCp/M where W_r is the sub-channel mass flow rate, Cp the specific heat of the fluid and M is the mixing coefficient between adjacent sub-channels. It is defined as the rate of heat transfer per unit length per unit temperature difference.

Consider two examples: the seven sub-channels case and the three-sub-channels case. Suppose that for each we wish to halve the temperature difference across the array at a distance l feet from inlet. This means we require a value of M, the mixing coefficient such that $7\,(W_rCp/M) = l$ for the seven sub-channels case and $1{\cdot}7\,(W_rCp/M) = l$ for the three sub-channels case. For an advanced gas-cooled reactor, the hottest point in the channel will be approximately 20 ft above the inlet; thus we can say that for significant mixing to occur right across the cluster we require a mixing coefficient M between adjacent sub-channels of about (7/20) W_rCp, but for significant mixing to occur between the centre and the outside we only require a mixing coefficient of (1·7/20) W_rCp.

Now $M = s \,.\, h_g$ where s is the gap width.

Thus

$$\frac{M}{W_rCp} = \frac{sSt_g}{A_f}$$

where A_f is the sub-channel flow area.

Typical values of s and A_f are 0·035 ft and 0·0055 ft^2.

Thus we have required values for St_g of 0·055 to give significant mixing right across the cluster and 0·013 to give significant mixing between the centre and outside. The values obtained for the rough cluster in the mixing tests is somewhat higher than 0·013 for the highest Reynolds number indicating that radial non-uniformities in temperature should be significantly reduced by mixing. It is unlikely that significant mixing will occur right across the cluster.

10. DISCUSSION

For the smooth cluster the measured rate of transfer through the gaps between rods is larger than can be accounted for by turbulent diffusion alone. However, measurements in other straight, smooth, non-circular ducts have indicated that secondary flows of about 2 per cent could occur in the gap region of a smooth cluster. Secondary flows of this order could account for the measured mixing rate. For the rough cluster, the measured mixing rate can be accounted for by a secondary flow in the gap region of about 6 per cent. This is considerably higher than any secondary flow rates that have been measured in straight smooth ducts, but because of the very high turbulence intensity occurring in roughened ducts, and because the secondary flows are caused by the turbulent fluctuations, it is not unreasonable to suggest that secondary flows of this magnitude could occur.

For the smooth cluster, the mixing rate, expressed as a gap Stanton number, falls off with increase in Reynolds number. This is to be expected as both turbulence intensity and secondary flow fall with rising Reynolds number. For the rough cluster, the gap Stanton number rises with increase in Reynolds number. This can be accounted for because at the fairly low Reynolds numbers of the tests the rough surface is not behaving as a fully roughened one. The friction factor was found to be rising at the lower Reynolds number end of the test range. It is reasonable to assume that the cluster is behaving as fully roughened at the highest Reynolds number and that the gap Stanton number will not rise any further. In fact the large rise in gap Stanton number for the rough cluster over the Reynolds number range tested is somewhat surprising, and as least confidence is held in the high Reynolds number results because of difficulty in obtaining good mass balances, the true gap Stanton number may be lower than shown for the highest value of Reynolds number. Measurements have shown that turbulence intensity remains constant with increasing Reynolds number for fully roughened surfaces, so one would expect the gap Stanton number to remain constant also at higher values of Reynolds number than those tested.

ACKNOWLEDGEMENTS

This paper is published by permission of the Central Electricity Generating Board, and is based on work carried out at Berkeley Nuclear Laboratories.

REFERENCES

1. W. B. HALL and J. H. HASHIMI, Heat transfer to a fluid in a circular pipe with a localised uniform source at the surface-mass transfer analogy, *Institution of Mechanical Engineers, Thermodynamics and Fluid Mechanics Group Symposium, Cambridge* (1964).
2. V. R. SKINNER, Measurements of flow mixing in a simple rod cluster by a new technique, *C.E.G.B. Rep.* No. RD/B/N677 (1966).
3. A. C. RAPIER, Forced convection heat transfer in passages with varying roughness and heat flux around the perimeter, *Institution of Mechanical Engineers, Thermodynamics and Fluid Mechanics Group Symposium, Cambridge* (1964).
4. J. NIKURADSE, *Ing.-Arch.* **1**, 306–332 (1930).
5. F. B. GESSNER and J. B. JONES, On some aspects of fully-developed turbulent flow in rectangular channels, *J. Fluid Mech.* **23**, 689 (1965).
6. L. C. HOAGLAND, Fully developed turbulent flow in straight rectangular ducts-secondary flow, its cause and effect on the primary flow, Doctor of Science thesis M.I.T. (1960).
7. E. BRUNDRETT and W. D. BAINES, The production and and diffusion of vorticity in duct flow, *J. Fluid Mech.* **19**, 375 (1964).
8. B. KJELLSTRÖM and S. HEDBERG, On shear stress distributions for flow in smooth or partially rough annuli, Aktiebolaget Atomenergi, Sweden Rep. No. AE-243 (1966).
9. K. HANJALIC and B. E. LAUNDER, Private communica- Imperial College TWF/TN/48 (1968).
10. J. LAUFER, The structure of turbulence in fully developed pipe flow, *NACA Tech. Rep.* No. 1174 (1954).

APPENDIX I

Determination of the Gap Stanton Number from Flow Mixing Results

Let the nitrous oxide flux diffusing from the inner sub-channel to the outer sub-channel through the rod gaps be n_g per unit area per second.

Then if diffusion has been taking place over an axial distance x*ft,

$$n_g s = -Q_1 \frac{\partial \bar{c}_1}{\partial x^*}. \tag{1}$$

Also from the definition of gap Stanton number,

$$St'_g = \frac{n_g}{\bar{\bar{u}}(\bar{c}_1 - \bar{c}_2)} \tag{2}$$

therefore,

$$(\bar{c}_1 - \bar{c}_2) = -\frac{Q_1}{\bar{\bar{u}} St'_g s} \frac{\partial c_1}{\partial x^*}. \tag{3}$$

Now the total quantity of nitrous oxide at any axial plane must be constant i.e. $Q_1\bar{c}_1 + Q_2\bar{c}_2 = (Q_1 + Q_2)\,\bar{\bar{c}}$ where $\bar{\bar{c}}$ is the overall channel concentration.

Eliminating $\bar{c}_2$ from equation (5) and replacing $\bar{\bar{u}}$ by $(Q_1 + Q_2)/A_f$ where A_f is the free flow area,

$$\int \frac{\partial \bar{c}_1}{(\bar{c}_1 - \bar{\bar{c}})} = -\frac{(Q_1 + Q_2)^2 s}{Q_1 Q_2 A_f} St'_g \int \partial x^*.$$

Let the value of $(\bar{c}_1 - \bar{\bar{c}})$ when $x^* = 0$ be $(\bar{c}_1 - \bar{\bar{c}})_0$

$$\log \frac{\bar{c}_1 - \bar{\bar{c}}}{(\bar{c}_1 - \bar{\bar{c}})_0} = -\frac{(Q_1 + Q_2)s}{Q_1 Q_2 A_f} St'_g x^*. \quad (4)$$

Now it can be shown that

$$\frac{\bar{c}_1 - \bar{c}_2}{(\bar{c}_1 - \bar{c}_2)_0} = \frac{\bar{c}_1 - \bar{\bar{c}}}{(\bar{c}_1 - \bar{\bar{c}})_0}.$$

Therefore the derived empirical relationship for concentration decay may be written

$$\frac{\bar{c}_1 - \bar{c}_2}{(\bar{c}_1 - \bar{c}_2)_0} = \frac{\bar{c}_1 - \bar{\bar{c}}}{(\bar{c}_1 - \bar{\bar{c}})_0} = e^{\gamma x^*} Re^{\alpha x^*}. \quad (5)$$

Hence,

$$St'_g = -\frac{Q_1 Q_2 A_f}{(Q_1 + Q_2)^2 s}(\gamma + \alpha \log_e Re). \quad (6)$$

Now

$$\frac{Q_2}{Q_1} = 1{\cdot}67 \text{ for the smooth cluster}$$
$$= 1{\cdot}70 \text{ for the roughened cluster.}$$

Substitution of values for A_f, s and Q_2/Q_1 gives:

$$St'_g = -0{\cdot}116(\gamma + \alpha \log_e Re).$$

APPENDIX II

Mixing between Adjacent Sub-Channels

In this Appendix, expressions are derived which show the effect of mixing on the temperature of gas flowing up arrays of up to seven adjacent sub-channels. The actual mechanism of mixing is not specified, but it is assumed that the rate of heat transfer, per unit length, between adjacent sub-channels is proportional to the bulk gas temperature difference between the channels.

To ease the analysis, a number of simplifying conditions have been taken, as follows:

(a) Equal mass flow rate along each sub-channel.
(b) Equal gas temperature, $\theta = 0$, at entry to each sub-channel.
(c) A uniform heat input rate along each sub-channel.
(d) A uniform heat input tilt across the array; thus if q_r is the heat input rate per foot into sub-channel r, q_{r+1} into sub-channel $r + 1$, then $q_r - q_{r+1}$ is constant.
(e) The rate of mixing, per unit temperature difference, between each pair of adjacent sub-channels is the same.

General case. Let $\theta_r(x)$ be the gas temperature at axial location (x) in channel r. Then using a superscript $'$ to signify differentiation with respect to x we get for channel r:

$$W_r Cp\theta'_r = q_r + M(\theta_{r-1} - \theta_r) - M(\theta_r - \theta_{r+1})$$

where W_r is the mass flow rate per channel, q_r the heat input rate per unit length for channel r, and M is the "mixing coefficient" per unit length. For channel $r + 1$ we get:

$$W_r Cp\theta_{r+1} = q_{r+1} + M(\theta_r - \theta_{r+1}) - M(\theta_{r+1} - \theta_{r+2}).$$

Subtracting these two equations, and writing:

$$\theta_r - \theta_{r+1} = \theta_{r,r+1} \text{ etc.}$$

we get:

$$\theta'_{r,r+1} = \frac{q_r - q_{r+1}}{W_r Cp} + \frac{M}{W_r Cp}(\theta_{r-1,r} - 2\theta_{r,r+1} + \theta_{r+1,r+2}).$$

By conditions (c) and (d) the first term on the right-hand side is independent of x and r. It is, in fact, the rate of increase in the x-direction of $\theta_{r,r+1}$ if no mixing occurs. Write:

$$\theta^* = \frac{q_r - q_{r+1}}{W_r Cp}.$$

The superscript* infers no mixing.

The term

$$\frac{M}{W_r Cp}$$

which has the dimensions of one over length, can be made numerically equal to unity by suitably choosing the unit of length. This has the

advantage of further simplifying the equation, giving:

$$\theta'_{r,r+1} = \theta^* + \theta_{r-1,r} - 2\theta_{r,r+1} + \theta_{r+1,r+2}.$$

In the following sections this expression is solved for three and seven adjacent sub-channels.

Three sub-channels. By symmetry we can say that:

$$\theta_{12} = \theta_{23}$$

therefore the general expression reduces to:

$$\theta'_{12} = \theta^* - \theta_{12}.$$

The solution is:

$$\theta_{12} = Ae^{-x} + \theta^*$$

and the boundary condition is: $\theta_{12} = 0$ at $x = 0$, giving $\theta_{12} = \theta^*(1 - e^{-x})$, and $\theta_{13} = 2\theta^*(1 - e^{-x})$.

The value of θ_{13} if no mixing occurs is $2x\theta^*$; therefore the reduction in θ_{13} brought about by mixing can be expressed:

$$\frac{\theta_{13}}{2x\theta^*} = \frac{1}{x}(1 - e^{-x}).$$

This is plotted in Fig. 13.

Seven sub-channels. Treating in a similar manner to the previous case we obtain eventually:

$$\theta_{17} = 2\theta^*[14 - 0{\cdot}010\,e^{-3{\cdot}247x} - 0{\cdot}145\,e^{-1{\cdot}555x} - 13{\cdot}844\,e^{-0{\cdot}198x}].$$

The value of θ_{17} if no mixing occurs is $6x\theta^*$ at axial position x; therefore the reduction in θ_{17} brought about by mixing can be expressed:

$$\frac{\theta_{17}}{6x\theta^*} = \frac{1}{x}[4{\cdot}667 - 0{\cdot}0033\,e^{-3{\cdot}247x} - 0{\cdot}0483\,e^{-1{\cdot}555x} - 4{\cdot}615\,e^{-0{\cdot}198x}].$$

This also is plotted in Fig. 13.

Résumé—Les différences transversales de température dans un réfrigérant s'écoulant axialement le long d'un groupe de barreaux ou un faisceau de tubes seront diminuées par la diffusion de la chaleur d'un sous-canal à un autre à travers les espaces entre les barreaux ou les tubes. Ce processus, appelé mélange par commodité a été étudié expérimentalement en employant une analogie de transport de masse. On a trouvé que les vitesses de mélange étaient plus grandes que celles expliquées par la théorie de la diffusion turbulente, ce qui a été attribué à l'action des vitesses secondaires. Les résultats sont employés à prédire à quel point le mélange réduira les différences de températures dans les groupes d'éléments combustibles des réacteurs modernes refroidis par gaz.

Zusammenfassung—Die Quertemperaturdifferenz in einem Kühlmittel, das längs eines Stab- oder Rohrbündels strömt, wird infolge des Wärmetransportes durch die Spalte zwischen den Stäben oder Rohren herabgesetzt. Dieser Vorgang, welcher einfachheitshalber Vermischung genannt sei, wurde experimentell unter Benutzung der Stofftransportanalogie untersucht. Die Vermischung erwies sich grösser, als durch die turbulente Diffusionstheorie erklärt werden kann. Dies wurde auf die Wirkung von Sekundärgeschwindigkeiten zurückgeführt. Die Ergebnisse werden herangezogen, um das Ausmass für die Herabsetzung der Temperaturdifferenz in den Brennstoffbündeln von fortgeschrittenen gasgekühlten Reaktoren zu bestimmen.

Аннотация—Поперечные перепады температур теплоносителя, продольно омывающего пакет стержней или труб уменьшаются за счет диффузии тепла от одной ячейки к другой через зазоры между стержнями или трубами. Этот процесс, называемый для удобства смешиванием, изучался экспериментально с привлечением аналогии массообмена. Найдено, что скорости смешивания больше величин, которые можно объяснить теорией турбулентной диффузии. Они определяются действием скоростей вторичных течений. Результаты используются для определения влияния смешивания на уменьшение перепада температуры в сборках твэлов усовершенствованных реакторов с газовым охлаждением.